LBL--12748

Conf-811012--54

Lawrence Berkeley Laboratory

UNIVERSITY OF CALIFORNIA

Engineering & Technical Services Division

Presented at the IEEE Nuclear Science Symposium, San Francisco, CA, October 21-23, 1981; and to be published in IEEE Transactions on Nuclear Science, Vol. NS-29, No. 1, February 1982

CARBON IN HIGH-PURITY GERMANIUM

E.E. Haller, W.L. Hansen, P. Luke, R. McMurray, and B. Jarrett

October 1981

LBL--12748

DE82 004550

Prepared for the U.S. Department of Energy under Contract W-7405-ENG-48

CARBON IN HIGH-PURITY GERMANIUM

LBL-12748

E. E. Haller**, W. L. Hansen*, P. Luke*, R. McMurray* and B. Jarrett*
*Lawrence Berkeley Laboratory and
**Department of Material Science and Engineering
University of California
Berkeley, California 94720 U.S.A.

Abstract

Using ^{14}C-spiked pyrolytic graphite-coated quartz crucibles for the growth of nine ultra-pure germanium single crystals, we have determined the carbon content and distribution in these crystals. Using autoradiography, we observe a rapidly decreasing carbon cluster concentration in successively grown crystals. Nuclear radiation detectors made from the crystals measure the betas from the internally decaying ^{14}C nuclei with close to 100% efficiency. An average value for the total carbon concentration $[^{14}C+^{12}C]$ is $\sim 2 \times 10^{14} cm^{-3}$, a value substantially larger than expected from earlier metallurgical studies. Contrary to the most recent measurement, we find the shape of the beta spectrum to agree very well with the statistical shape predicted for allowed transitions.

Introduction

Pure and doped germanium single crystals have traditionally been grown from a melt contained in a graphite susceptor . Graphite combines several electrical and chemical properties which are advantageous for its use as a susceptor material. It couples well to a RF heater coil, it can be purified with a high temperature chlorine gas process which removes most metallic impurities to negligible levels, and a graphite susceptor does not introduce undesirable oxygen to the crystal growing apparatus. Graphite is, in the metallurgical sense, not miscible with germanium near the melting point of the latter.[1] The meaning of this for a pure semiconductor will be examined below. In the course of developing ultra-pure germanium single crystals for the fabrication of nuclear radiation detectors,[2] it was found that the purest graphite still contained unacceptable levels of boron and phosphorus. Lining the graphite susceptor with a synthetic quartz crucible led to the necessary net-dopant levels of $< 2 \times 10^{10} cm^{-3}$ [3] From this point on the interest in graphite in relation to the development of ultra-pure germanium dropped.

The recent discovery of a large number of novel acceptor and donor centers in high-purity germanium has refocused the attention to several impurities which have been completely neglected in the past because they are neutral by themselves. Hydrogen, oxygen, silicon and carbon have been found to form impurity complexes, some of which can act as donors, others as acceptors.[4] With concentrations often well above the concentration of the residual elemental acceptors such as boron, aluminum, gallium, etc. or donors such as phosphorus, arsenic, lithium, etc., these new centers can play a very detrimental role. Hall[5] discovered the first two of these unknown centers in hydrogen atmosphere, quartz-crucible-grown crystals when he rapidly cooled crystal samples from $T = 400^{\circ}C$ down to room temperature. Temperatures in this range are routinely used for the formation of p^+ contacts by lithium diffusion. Hall's centers along with several other novel acceptor levels have been explored using Photothermal Ionization Spectroscopy and doping experiments.[4] A simple model which can explain all the observed properties of several of the new centers has been proposed recently.[5] The model is based on a heavy, substitutional impurity such as copper, oxygen, silicon or carbon trapping a light, interstitial impurity such as hydrogen or lithium in its vicinity (Fig. 1). The potential well which is trapping the interstitial impurity is thought to be created by the difference in the bond length of the substitutional impurity and the germanium host lattice. The "rapid quench" centers (as Hall called them) fit the above model and have been named according to their composition A(H,Si) and D(H,C) (A stands for acceptor, D for donor). Detector makers can avoid the formation of these undesirable centers by cooling slowly after any heating cycle, better even by keeping the device at $T = 160^{\circ}C$ for 10 to 30 minutes before returning to room temperature.

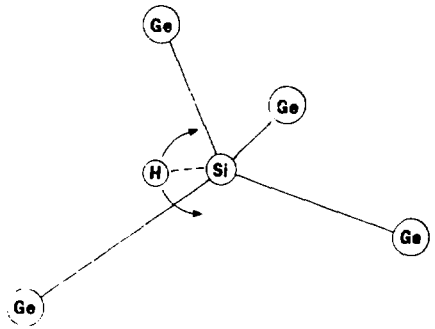

Fig. 1. Sketch of the Si-H acceptor complex A(H,Si) in germanium. The silicon impurity resides in a substitutional position and the interstitial hydrogen atom tunnels in its vicinity.

Another novel acceptor with properties very similar to A(H,Si) though not as abundant, has been linked to hydrogen and carbon. Called A(H,C) it also appears upon rapid quenching but remains stable up to temperatures $T = 200^{\circ}C$. The determination of its composition has not been as unambiguous as in the case of A(H,Si). The reason for the ambiguity lies in the very limited knowledge about the solubility of carbon in germanium. Scace and Slack[7] concluded from measurements between 2800 and 3200°C that the solubility of carbon should be at least $10^{18} cm^{-3}$ at the germanium melting point ($T = 937^{\circ}C$), an extremely small concentration indeed! This far extrapolation carries, however, a very large error and is therefore far too unreliable to be useful. Because the concentration of A(H,C) can be as high as $\sim 10^{12} cm^{-3}$ after rapid quenching, we have to assume that at least 10^{12} carbon cm^{-3} must be present in some ultra-pure Ge crystals.[6]

Though ultra-pure germanium crystals are grown from melts contained in synthetic quartz crucibles, it has not been known before this study how much of the carbon which is present in all the commercially available germanium carries over through the various additional processes to the final product. In this paper we present the first experimental results on the solubility of carbon in germanium and the propagation of carbon through the crystal growth process using quartz crucibles. Because of the large uncertainty in the available concentration data, we decided to use a radioactive tracer technique. Carbon 14 is a convenient radioactive isotope for the study of carbon chemistry. The half life of ^{14}C is $T_{1/2} = 5730$ years. This is very long for all practical purposes. The maximum beta energy is $E_{max} = 156$ keV.[8]

Experimental

A Novel Radioactive Tracer Technique

One of the standard radioactive tracer techniques uses the exposure of x-ray film by the betas (nuclear electrons) emitted during the decay of a radioactive isotope. This technique, called autoradiography[9] has excellent spacial resolution. For isotopes with small maximum beta energy (carbon 14 and tritium belong to this group), autoradiography is limited to thin specimens because of source self absorption. In addition, autoradiography lacks sensitivity and gives only semi-quantitative results. These shortcomings are of no importance in the study of biological metabolisms[9] or for the detection of carbon during the production of silicon using the pyrolysis of trichlorosilane.[10] In both of these cases the concentration of carbon is very high compared with the concentration we may expect to find in germanium crystals.

The radioactive tracer technique can be made ultra-sensitive, quantitative and isotope specific by making use of a truly unique opportunity. The semiconductor crystals which we want to analyze with carbon 14 are sufficiently pure that samples can be made into nuclear radiation detectors. Because the maximum range of the ^{14}C beta particles is small ($r_{max} \sim 150$ um) compared with the detector dimensions, the betas are detected with close to 100% efficiency. The energy of each internally emitted beta particle can be measured and stored in a pulse height analyzer. The beta spectrum shape and end-point energy are isotope specific and the integral over the spectrum divided by the counting time and the detector volume gives the decay rate per unit volume $\frac{dN}{dt}$. Using the radioactive decay equation:

$$\frac{dN}{dt} = -\frac{\ln 2}{T_{1/2}} N \qquad (1)$$

with the half life of carbon 14 $T_{1/2} = 5730$y, we can determine the concentration N of ^{14}C.

^{14}C Labeling of High-Purity Ge Crystals

Germanium crystals grown from a melt contained in a pyrolytic graphite-coated quartz crucible will be saturated with carbon. It has been shown that such crystals are identical to bulk graphite-grown crystals.[2] Spiking of the pyrolytic graphite coating with carbon 14 can therefore be used to label germanium crystals.

Pure ^{14}C- methane (100 m Curie) was mixed with stable ^{12}C methane (7% in argon) in a stainless steel tank (150 cm^3) by cryogenic transfer at liquid nitrogen temperature (T = 77 K). The ratio of $[^{12}C]$ to $[^{14}C]$ in the gas mixture is 10.33. The mixture was introduced into a quartz reaction chamber (Fig. 2) which contained the quartz crucible at T = 1050°C. A gas flow of 75 cm^3 per minute was chosen. The methane pyrolyzes at this temperature and the free carbon coats all the surfaces inside the reaction chamber. The gas exhaust was guided through a three-foot-long quartz tube filled with CuO needles inside a tube furnace at T = 600°C in order to transform all the hydrogen and carbon to water and carbon dioxide. The latter were absorbed quantitatively in a ascarite II[18] cell in order to keep any radioactive carbon trapped. A coating time of 20 minutes led to a ~ 4000Å thick graphite layer on the inside of the quartz crucible as determined by weighing. The formation of some carbon particles could not be avoided completely and this may be the source of the carbon particles which are present in most of our ^{14}C labeled crystals. Two synthetic quartz crucibles were coated with ^{14}C labeled graphite.

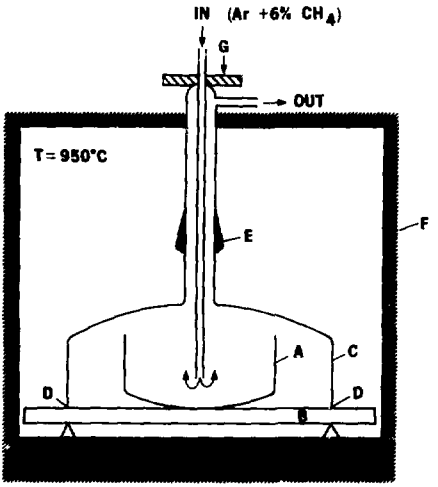

XBL 7511-8935

Fig. 2. Furnace used for pyrolytic carbon coating of quartz crucibles; A=crucible, B=quartz base plate, C=quartz cover with a ground joint at D and E, F=furnace, G=weight which keeps the joints tight.

Seven crystals were grown in a hydrogen and one in a nitrogen atmosphere from melts contained in the coated crucibles. One other crystal was grown in a standard suprasil quartz crucible using a ^{14}C-labeled crystal as a starting charge. The axes of all crystals are parallel [113]. The crystal growing process has been described in detail.[3] Because pyrolytic graphite-crucible-grown crystals are in general all p type with the major impurity aluminum segregating towards the tail end of the crystal, we lightly counterdoped some of the ^{14}C-labeled crystals with n-type germanium. In this way, it became

possible to obtain crystals with p-n junctions, i.e., regions with very low net-dopant concentrations $|N_A - N_D|$.

Results

Internal Beta Decay Detection

A number of nuclear radiation detectors[11] were produced from the ^{14}C labeled crystals. A few devices reached full depletion, others could only be partially depleted. The depletion depth of the latter ones was determined from the capacitance and the detector area. The beta spectra were accumulated and stored in a multichannel pulse height analyzer. A typical spectrum is shown in Fig. 3. The shape of the spectrum deviates at low energies from a "statistical" spectrum which should be observed according to Fermi's beta decay theory.[12] With an electronic resolution of about 2 keV FWHM, we expect electronic pulses up to ~ 7 keV. Incomplete charge collection of betas stopped inside or close to the lithium diffused n^+ contact, near the detector periphery and near the boron-implanted p^+ contact lead to pulses with reduced amplitude and to a distortion of the spectrum mainly at low energies.

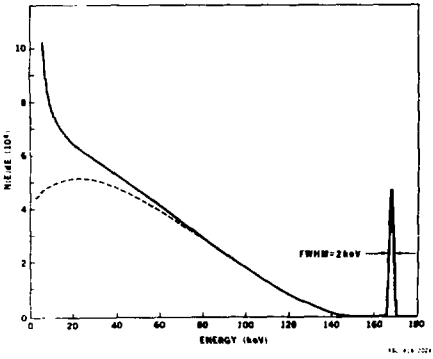

Fig. 3 Carbon 14 beta decay spectrum recorded with an undepleted detector. Incomplete charge collection from events occurring in the thick n^+ contact layer, rear bare surfaces and the thin p^+ contact lead to an increased pulse rate at low energies. The dashed line follows the shape of a "statistical" spectrum for Carbon 14. Detector #680-10.3 was biased with 1500V which produces a 5.1 mm wide depletion layer, $N_A-N_D=1x10^{11}cm^{-3}$.

Recording two spectra at different biases which do not deplete the detector, and subtraction of the lower bias spectrum from the higher bias spectrum substantially reduces the shape distortion (Fig. 4). Integration over the upper third of all three spectra yield, however, very similar beta decay rates per unit volume. This means that the shape distortion is negligible in the upper third of the spectrum. The strong energy dependence of shape distortions can be understood when one assumes that any given fractional charge collection loss occurs with a constant probability for any given beta energy. This assumption is experimentally supported by measurements of monoenergetic internal conversion electrons. Such spectra

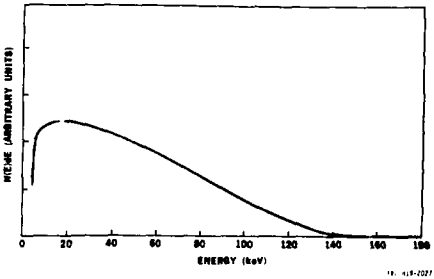

Fig. 4. Difference spectrum obtained from spectra recorded at 2000 and 1000 V bias. The same detector as in Fig. 3 was used. Note the reduction in the net low energy pulse rate.

generally show an energy independent increase in the background below each electron peak. Table 1 contains a summary of all the results obtained from the analysis of internally detected beta spectra. Disregarding details, it becomes clear that the carbon concentration in our crystals is by many orders of magnitude larger than the lower limit predicted by Scace and Slack. If we exclude the first crystal #678 because of the large carbon cluster content, and the last crystal #701 because it has been a second generation crystal grown in a bare quartz crucible, we obtain an average value for the total carbon concentration of $2.5x10^{14}cm^{-3}$ at about one third of the melt frozen.

In order to determine the segregation coefficient of carbon in germanium, fully depleted detectors were made from slices taken at three different positions along the length of the second generation crystal (#701). The experimental points show a clear decrease in the carbon concentration along the crystal length (i.e. with increasing % of melt frozen). This implies a segregation coefficient greater than unity as in the cases of boron and silicon in germanium. A good theoretical fit to the experimental points was obtained with an effective segregation coefficient of $k_{eff}=1.85$ (Fig. 5). Our data on crystal #683, though not as accurate as for crystal #701 show the same dependence of the carbon concentration on the % of melt frozen. This result is compatible with the tentative phase diagram Ge -C which indicates a rise of the melting point with increasing carbon fraction.

Autoradiography

Two 2 mm thick slices from each crystal, one near the seed end and one near the tail end were cut, lapped and polish etched. Four slices were sandwiched between two 5 x 5" sheets of Kodak SB5 x-ray film. The small black spots in Fig. 6 were produced by a continuous three months exposure of the slices from crystal #682. They indicate carbon clusters. The original film sheet shows a barely detectable increase in general background exposure between the spots compared with the unexposed areas of the film. We assume that this increase is due to the substitutionally dissolved carbon atoms. Figure 7 shows autoradiographs of the nitrogen-atmosphere-grown crystal #685. Several noteworthy differences can be detected.

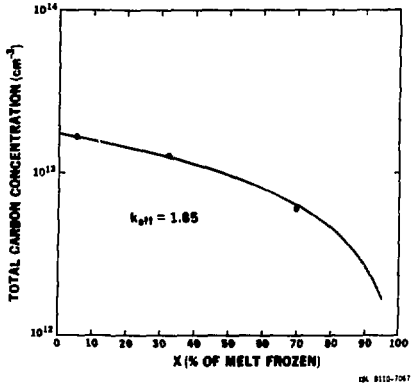

Fig. 5. An effective segregation coefficient k_{eff}=1.85 gives the best fit to the carbon concentration in function of % melt frozen.

The crystal sample taken near the tail end contains virtually no carbon clusters. A clearly visible exposure above background has occurred. The sample from near the seed end shows two additional features. Enhanced exposure occurred near the (111) facets close to the crystal slice periphery. A similar facet effect has been observed by Martin and Haas in silicon single crystals produced by the pyrolysis of trichlorosilane.[10] The effect only appeared when ^{14}CO was used as a carbon marker. The second much more subtle observation which can be made on the original autoradiograph is a generally lighter exposure within a zone extending 2 mm from the periphery inwards.

Experiments are in progress which should lead to the concentration and probably the relative size of the carbon clusters in hydrogen-atmosphere-grown crystals. A sequence of autoradiographs, each one exposed for three days, will be recorded. In between each exposure a thin layer between 10 and 30 μm thick will be etched off both sides of the Ge wafers. Careful comparison of the autoradiographs will show how many clusters appear and how many disappear after each etching cycle.

Discussion

The results reported in the previous section cannot be regarded as final. Much more work is needed to understand the chemistry of carbon in germanium. Our experiments have, however, clarified a very important point. There is obviously much more carbon in ultra-pure crystals than was expected. The carbon concentration is high enough to be compatible with our model for a carbon related acceptor A(H,C). A surprising result is the fact that regrowing a crystal in a quartz crucible reduces the carbon concentration only by a factor of ~30. We would have expected that the reduction of quartz would provide enough oxygen to transform all the carbon into volatile carbon monoxide or dioxide. This is clearly not the case. Further crystal growing experiments will show how the carbon propagates through more crystal growth generations. The presence of clusters raises an unanswered question. How much carbon resides in clusters and

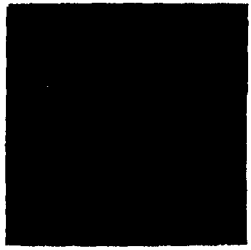

Fig. 6. Autoradiograph from two slices of the hydrogen-atmosphere-grown crystal #682. The small black dots indicate the presence of carbon clusters and not individual beta tracks. The flared dots near the upper edge of 682-7.3 are due to carbon clusters on the crystal surface.

how much is dissolved atomically in the lattice? A final answer could be obtained if one could detect the lattice vibrations of carbon in the germanium lattice. Lattice vibrations have been found by infrared absorption for oxygen in silicon[13] and germanium,[14] and for carbon in silicon.[15] The detection limit for the ir-absorption technique lies around 10^{14} to $10^{15}cm^{-3}$. This means that we are working just at the limit of detection in the case of carbon in germanium. The observation that the concentration of carbon clusters is decreasing with crystals successively grown out of the same crucible while the ^{14}C beta decay rate remains constant after the first crystal indicates that most of the carbon is dissolved atomically and does not reside in clusters. This is certainly true for the nitrogen-atmosphere-grown crystal which contains virtually no clusters. The differences in the autoradiographs of hydrogen- and nitrogen-atmosphere-grown crystals is another interesting point which we cannot understand quantitatively at

the present time. We assume that the difference in the oxygen partial pressure plays an important role. Further support of this assumption comes from the observation that the nitrogen-atmosphere-grown crystal did not show any beta activity on its as-grown surface while all the hydrogen-atmosphere-grown crystals exhibited high surface activities.

A further, incidental result has been obtained with a detector made from the second generation ^{14}C-labeled crystal #701. This crystal is pure enough so that a thick detector could be fully depleted. Using an active guard ring working as an anticoincidence counter, we have obtained beta spectra with a shape which is very close to the ideal statistical spectrum of an allowed transition. Our detector and counting configuration simulates an infinitely large or "surface free" detector. We do not have to apply any corrections to the raw data. Figure 8 shows a ^{14}C beta spectrum and Fig. 9 displays the corresponding Fermi-Curie plot. The latter is expected to fit a straight line if the spectrum follows the statistical shape. A best fit to the data between ~ 30 keV and E_{max} leads to a value of the maximum beta energy of 155.06 ± .10 keV. Our results for the shape of the beta spectrum are in strong disagreement with the most recent data published by Sonntag et al.[16] This group detected a substantial deviation from the ideal spectrum shape at low energies and used this finding to explain the anomalously long half life of ^{14}C. We feel that our data which are free of any corrections may represent the true shape of the ^{14}C beta spectrum more closely. Furthermore we find that the older data[17] are also in closer agreement with the ideal spectrum than the results by Sonntag et al.

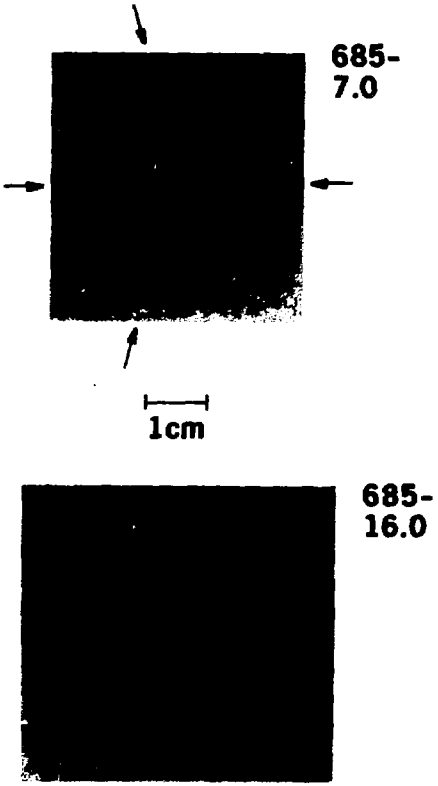

Fig. 7. Autoradiograph of two slices of the nitrogen-atmosphere-grown crystal #685. The carbon cluster content is very small. The seed end slice shows enhanced carbon cencentration near the (111) facets. A large carbon particle on the crystal surface produced the flare in the lower autoradiograph (685-16.0).

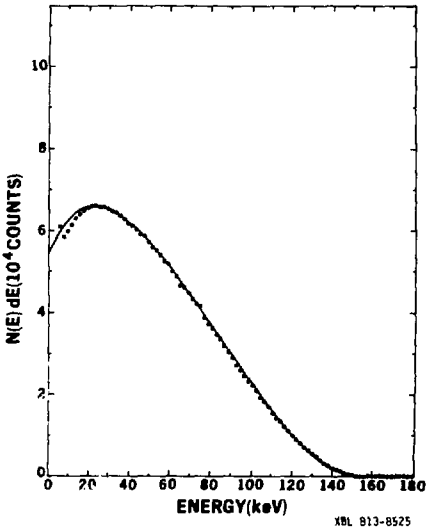

Fig. 8. Carbon-14 beta spectrum obtained with a fully depleted detector (701-13.2) and an active guard ring working in anticoincidence. Only every 20th point of the spectrum is displayed. The solid line corresponds to the "statistical" spectrum of the allowed $^{14}C \rightarrow {}^{14}N+\beta$ transition.

Acknowledgments

We would like to thank B. Gordon, Melvin Calvin Lab, U.C. Berkeley for his extensive assistance in setting up the carbon 14 pyrolytic coating apparatus. F.S. Goulding has contributed with many discussions and with continued interest in this work.

This work was supported in part by the Director's Office of Energy Research, Office of Health and Environmental Research, Pollutant Characterization and Safety Research Division of the U.S. Department of Energy under Contract No. W-7405-ENG-48.

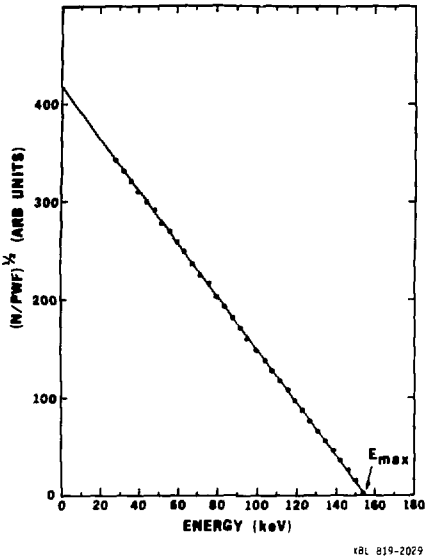

Fig. 9. Fermi-Curie plot f - the spectrum in Fig. 3.

References

1. Hansen M and Anderko K, Constitution of Binary Alloys, MacGraw Hill Co., New York (1958).

2. Haller E E, Hansen W L, Hubbard G S and Goulding F S, IEEE Trans. Nucl. Sci. NS-23, No. 1, 81 (1976).

3. Hansen W L, Nucl. Instr. Meth. 94, 377 (1971); and Hall R N and Seltys T J, IEEE Trans. Nucl. Sci. NS-18, No. 1, 160 (1971).

4. For a review see: Haller E E, Hansen W L and Goulding F S, Adv. in Physics 30, No. 1, 93 (1981).

5. Hall R N, Inst. Phys. Conf. Ser. 23, 190 (1975).

6. Haller E E, Joós B and Falicov L M, Phys. Rev. B21, 4729 (1980).

7. Scace R I and Slack G A, J. Chem. Phys. 30, 1551 (1959).

8. Table of Isotopes (7th ed.) eds. Lederer C M and Shirley V S, J. Wiley and Sons, Inc., New York (1978).

9. Rogers A W, Techniques of Autoradiography (3rd ed.) Elsevier/North Holland Biomedical Press, Amsterdam (1979).

10. Martin J and Haas E, Sol. State Elec. 11, 993 (1968).

11. See for example: Haller E E and Goulding F S, Handbook on Semiconductors, Vol. 4, Ch. 6C, 799, ed. Hilsum C, North Holland, New York (1981).

12. Fermi E, Nuovo Cimento 11, 1 (1934); and Fermi E, Z. Phys. 88, 161 (1934); also Wu C S, "The Shapes of Beta-Spectra" in Alpha-, Beta- and Gamma-Ray Spectroscopy, Vol. 2, ed. Siegbahn K, North Holland Publ. Co., Amsterdam (1965).

13. Pajot B, Analusis 5, No. 7, 293 (1977).

14. Millett E J, Wood L S and Bew G, Brit. J. Appl. Phys. 16, 1593 (1965).

15. Bean A R and Newman R C, J. Phys. Chem. Solids 32, 1211 (1971).

16. Sonntag C, Rebel H, Ribbat B, Thio S K and Gramm W R, Lett. Nuovo Cim. 1V, 717 (1970).

17. Moljk A and Curran S C, Phys. Rev. 96, 395 (1954).

18. A. H. Thomas Co., Philadelphia, PA. Catalog No. C049-440.

Table 1.

Crystal #	Crystal Growth Atmosphere	Detector Position x (x=% of melt frozen)		Total Carbon Concentration (cm^{-3}) $[^{14}C] + [^{12}C]$	Comments
678	H_2	15	nd*	$(4.5 \pm 2.0) \times 10^{15}$	very high carbon cluster content
680	H_2	50	fd*	$(2.4 \pm 0.3) \times 10^{14}$	some carbon clusters
681	H_2	13	fd	$(6.7 \pm 0.7) \times 10^{14}$	some carbon clusters
682	H_2	35	nd	$(3.0 \pm 0.6) \times 10^{14}$	some carbon clusters
683	H_2	2	nd	$(2.3 \pm 0.5) \times 10^{14}$	some carbon clusters
		65	fd	$(1.0 \pm 0.1) \times 10^{14}$	some carbon clusters
685	N_2	44	nd	$(3.0 \pm 0.15) \times 10^{14}$	practically no carbon clusters
701	H_2 quartz crucible, regrowth of crystal #6	87	fd	$(5.9 \pm 0.03) \times 10^{12}$	no carbon clusters, guard-ring reject detector

*nd = not depleted, fd = fully depleted